MINERALOGICAL EXAMINATION OF THE YAMATO-75 ACHONDRITES AND THEIR LAYERED CRUST MODEL

Hiroshi TAKEDA,

Mineralogical Institute, Faculty of Science, University of Tokyo, Hongo 7-chome, Bunkyo-ku, Tokyo 113

Masamichi MIYAMOTO,

Department of Earth Sciences, Kobe University, Rokkodai-cho, Nada-ku, Kobe 657

Teruaki ISHII,

Ocean Research Institute, University of Tokyo, Minamidai, Nakano-ku, Tokyo 164

Keizo YANAI

National Institute of Polar Research, Kaga 1-chome, Itabashi-ku, Tokyo 173

and

Yukio MATSUMOTO*

Department of Geology, Faculty of Liberal Arts, Nagasaki University, 1–14, Bunkyo-machi, Nagasaki 852

Abstract: One Fe-rich diogenite and two polymict breccias with eucritic composition have been identified in the Yamato-75 achondrites by the electron microprobe and single crystal X-ray diffraction techniques. The Yamato-75032 diogenite, a monomict breccia, contains a low-Ca inverted pigeonite with a chemical composition close to that of Binda, and a possible primary orthopyroxene. Yamato-75011 and -75015 are polymict breccias which contain mineral and lithic clasts common to eucrites. Binda-like pyroxene fragments were found in Yamato-75015, suggesting that it may represent a variety of materials expected from our layered crust model containing diogenite, Binda-type, Moore County-type, Juvinas-type and Pasamonte-type pyroxenes from bottom to top. Yamato-74659 may be classified as a weathered pyroxene-rich ureilite, which contains the most Mg-rich uninverted pigeonite. The exsolution and shock induced twinning were not observed. Yamato-74123 is another ureilite similar to Kenna.

1. Introduction

The achondrites found in the Yamato meteorite collection include one diogenite in Yamato-69 (b) (OKADA, 1975; TAKEDA *et al.*, 1975), one howardite in

* Present address: Department of Mineralogical Science and Geology, Faculty of Science, Yamaguchi University, 1677–1, Yoshida, Yamaguchi 753.

Table 1. List of the Yamato achondrites studied to date.

No.	Original weight (g)	Dimension (cm)	Date of found	Remarks
Yamato				
-692(b)	138	(5.6×3.9)	Dec. 21, 1969	Diogenite
-74010	298.5	7.0×6.5	Nov. 25, 1974	〃
-74011	206.0	6.5×5.0	〃	〃
-74013	2059.5	15×10	〃	〃
-74037	591.9	8.6×8.2	Nov. 27, 1974	〃
-74097	2193.9	16×11	Dec. 2, 1974	〃
-74136	725.0	9.0×7.0	Dec. 4, 1974	〃
-74648	185.5	5.7×4.0×3.5	Dec. 28, 1974	〃
-75032	189.1	5.5×6.0	Dec. 7, 1975	〃
-7308(l)	480	9.0×7.5×4.5	Dec. 22, 1973	Howardite
-74159	98.2	8.6×3.6	Dec. 8, 1974	Eucritic polymict breccia
-75011	121.5	7.1×4.4	Dec. 1, 1975	〃
-75015	166.6	7.0×4.5	〃	〃
-74450	235.6	5.5×5.5	Dec. 23, 1974	Eucrite
-74044	51.8	4.7×3.0	Nov. 27, 1974	Pallasite
-74123	69.9	4.5×3.0	Dec. 3, 1974	Ureilite
-74659	18.9	4.2×2.7	Dec. 29, 1974	〃

Yamato-73 (l) (TAKEDA *et al.*, 1976; YAGI *et al.*, 1978; MIYAMOTO *et al.*, 1978); seven diogenites, one eucritic polymict breccia (MIYAMOTO *et al.*, 1978), one eucrite and one pallasite (TAKEDA *et al.*, 1978a) in Yamato-74. A brief catalogue of these meteorites is given in Table 1. A preliminary examination of the Yamato-75 meteorites (MATSUMOTO, 1978) revealed one iron-rich diogenite and two eucritic polymict breccias. Mineral chemistry and pyroxene crystallography of these three Yamato-75 achondrites have been investigated by electron microprobe and X-ray diffraction techniques. The bulk chemistry and mineralogy of two new ureilites, Yamato-74659 and -74123 collected in 1974 are also described in this paper.

The results have been interpreted in light of the recent developments concerning the parent body model of achondrites (MATSON *et al.*, 1976; DRAKE and CONSOLMAGNO, 1977), especially a layered crust model (TAKEDA *et al.*, 1976). The asteroid 4 Vesta shows a unique reflectance spectrum which matches that of the basaltic achondrites. It appears to be the only good candidate in the solar system for the parent body of these meteorites. LEBERTRE and ZELLNER (1978) concluded that the polarization-phase curve of Vesta can be explained by crushed basaltic achondrites with a substantial component of very fine dust. Thus, eucritic polymict breccias found in the Yamato meteorites may provide information on

the surface materials of such an asteroid.

The presence of inverted pigeonites with blebby augite elongated along the *c*-axis with (100) in common with the host orthopyroxene have been reported for the cumulate eucrites Binda and Moama (TAKEDA *et al.*, 1976). Their low-Ca contents have been attributed to producing such textures and their significance and a possible unmixing process has been pointed out (TAKEDA and MIYAMOTO, 1977) in conjunction with pyroxene-crystallization trends in achondritic crusts. A preliminary examination of the Yamato-75032 and -75015 has indicated that these meteorites also contain such pyroxenes (TAKEDA *et al.*, 1978a). Yamato-75032 is the most Fe-rich diogenite. If these pyroxenes were originally pigeonites with low-Ca concentration, it would imply that this diogenite contained pigeonite in addition to orthopyroxene. A presence of the Binda-like pyroxene in Yamato-75015 suggests that this breccia contains entire samples of the eucritic crust. In order to clarify these points and to understand the pyroxene-crystallization trends of an achondritic crust, we investigated Yamato-75032 and -75015 in more detail.

2. Experimental Techniques

The methods we used are the same as those described in a previous paper (TAKEDA *et al.*, 1978a). Several small polished grain mounts of Yamato-75011 and -75015 prepared previously were reinvestigated. An epoxy mount (potted butt) of Yamato-75032 prepared previously from about one half of the original 1.0 g chip was sliced to produce four polished sections. A few single crystals of pyroxene were separated for X-ray diffraction studies. A 0.065 g chip of Yamato-75011 was mounted in epoxy resin, and three polished thin sections were prepared.

A newly cut fragment (1.881 g) of Yamato-75015 supplied from the National Institute of Polar Research had one flat cut face and the other sides are round and are covered by a black shiny fusion crust. One large polished thin section of the above cut surface, 1.9×1.3 cm in size was prepared, and a small cut block $1.4 \times 0.5 \times 0.5$ cm was mounted in epoxy resin, and four thin sections were sliced perpendicular to the above large cut surface. One polished thin section of each meteorite was cemented by araldite and regular polished thin sections were produced for microprobe analyses. The others were cemented by Stick-wax and were finished to about 0.1 mm thick so that single crystals of particular compositions could be separated after microprobe analyses.

The quantitative chemical analyses were made with a JOEL JXA-5 electron probe X-ray microanalyzer with a 40° take-off angle. The method is the same as that of NAKAMURA and KUSHIRO (1970). The pyroxene crystals were mounted approximately along the *c*-axis, and were aligned with spindle axis parallel to the c^* direction. Precession photograph of $h0l$ nets were taken using Zr-filtered Mo $K\alpha$ radiation.

3. Diogenites

3.1. Results

As was reported previously, the Yamato-75032 meteorite is the only unrecrystallized monomict Yamato diogenite. The meteorite is composed of translucent white crystals set in a dark glassy matrix in hand specimen. The bulk chemical composition of Yamato-75032 (Analysis by H. HARAMURA; TAKEDA *et al.*, 1978a) is the most iron- and calcium-rich among the known diogenites. Its composition approaches that of the most magnesium-rich eucrite, Binda.

In order to demonstrate the similarity of the pyroxenes between Yamato-75032 and the Mg-rich eucrites, we cite observations on the Binda and Moama pyroxenes. Microscopic observation of the thin sections and polished single crystal mounts, for which the orientation of the crystals are known, confirm that many blebby inclusions of augite are elongated along the *c*-axis of augite and that the host orthopyroxene was inverted from pigeonite with (100) in common. Good examples of such orientational relationships are exemplified by photomicrographs of the Moama and Binda inverted pigeonites (Fig. 1). The blebby inclusions which parallel the *c*-axes resembles platy exsolution lamellae (Fig. 1), but the section cut perpendicular to the lamellae confirms that the blebs are rods, elongated slightly along one direction. A few augite blebs in Moama share common (001) with the original pigeonite, but they are not platy (001) lamellae

a. Moama eucrite. Width is 2 mm. Thin section supplied from Prof. J. F. LOVERING.

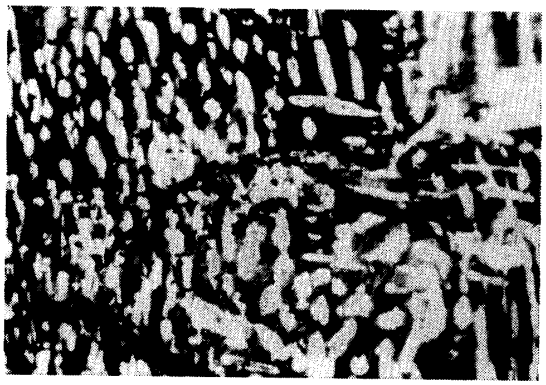

b. Binda, the most Mg-rich eucrite. Width is 0.73 mm. Photograph courtesy of Prof. A. M. REID of the University of Cape Town.

Fig. 1. Photomicrographs (crossed nicols) of low-Ca inverted or decomposed pigeonites. Blebs of augites are elongated along the c-axis.

Fig. 2. Photomicrograph (crossed nicols) of a low-Ca inverted pigeonite in Fe-rich diogenite, Yamato-75032. Augite blebs are elongated along one direction. Width 0.7 mm.

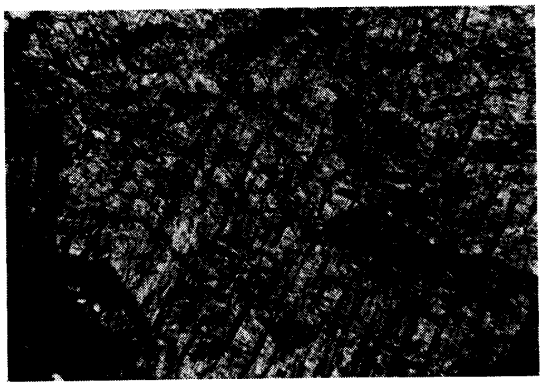

Fig. 3. Host orthopyroxene with regularly spaced lamellae-like augites accompanied by opaque mineral inclusions in Yamato-75032. Width 1.1 mm.

Fig. 4. A possible primary orthopyroxene with fine augite exsolution lamellae in Yamato-75032. Width 0.95 mm. c-axis horizontal.

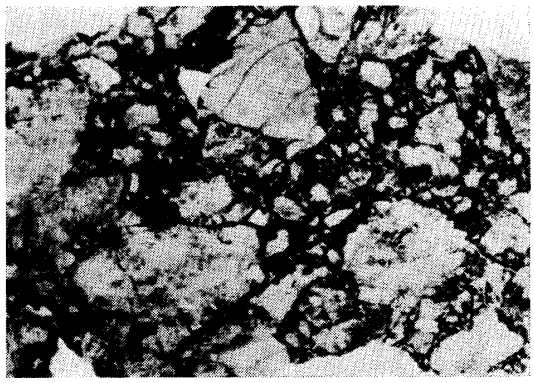

Fig. 5. Photomicrograph (open nicols) showing the texture of a monomict breccia, the most Fe-rich diogenite, Yamato-75032. The matrix between the mineral clasts are dark colored glassy. Width 5.0 mm.

known from common inverted pigeonites (TAKEDA and MIYAMOTO, 1977). The characteristics of the X-ray diffraction patterns of the above two orientations were described previously (TAKEDA *et al.*, 1976).

The orientational relationships of augite and orthopyroxene in Yamato-75032 are not as straightforward as those of Moama and Binda. In one crystal, augite blebs are elongated along one direction (Fig. 2). In some crystals, however, augites are present as coarsely separated (100) lamellae, and in some other crystals regularly spaced lamellae-like augites are found (Fig. 3). Electron microprobe traverse by monitoring Ca, Mg, Fe $K\alpha$ radiation, detected the presence of very fine augite lamellae between the coarse ones. There is, however, another type

of orthopyroxene, which shows very fine lamellae of augite with (100) in common (Fig. 4) as a fragment in the monomict breccia (Fig. 5). This texture is very similar to the exsolution patterns of a primary orthopyroxene (ISHII and TAKEDA, 1974). In addition, the bulk Ca contents (atomic ratio) of such orthopyroxene (Table 2), Ca/(Ca+Mg+Fe)=0.03–0.04 (Fig. 6), is somewhat higher than that of the host orthopyroxene (0.015–0.03) of the grains containing the blebby augite (Fig. 6). The orthopyroxene grains with augite blebs have much higher bulk Ca contents (0.04–0.07). The Fe/(Mg+Fe) atomic ratios of the pyroxenes range from 0.31 to 0.37. The dominant composition of the primary orthopyroxenes are slightly more Mg-rich than that of the orthopyroxene with blebby augites, possibly an inverted pigeonite.

The dark matrix filling interstices of the pyroxene clasts (Fig. 5) displays the same bulk chemistry as that of the bulk pigeonites, but the calcium content is

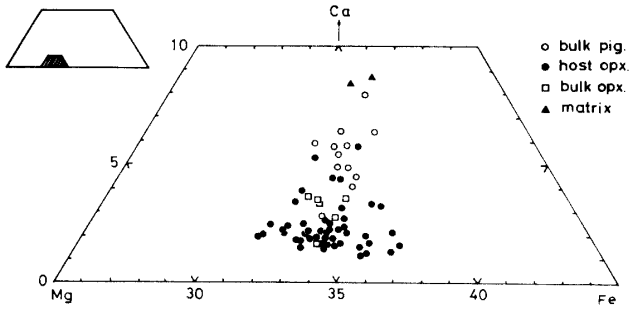

Fig. 6. Enlarged pyroxene quadrilateral of the small shaded area of the Yamato-75032 pyroxenes.

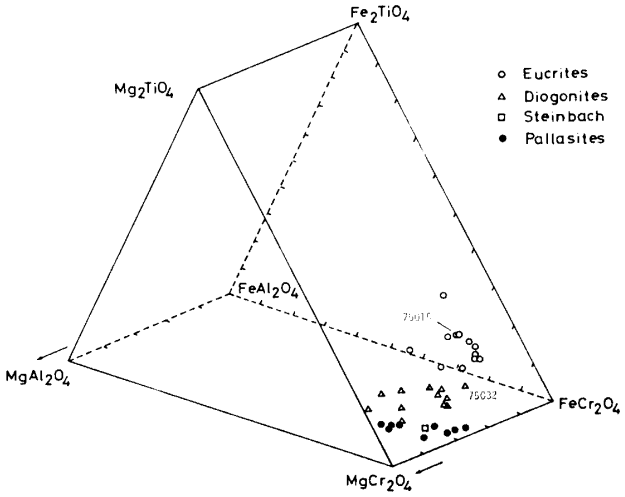

Fig. 7. Generalized compositional trends in the chromite from various achondrites. Yamato-75032 chromite is intermediate between those of diogenites and eucrites.

Table 2. Selected pyroxene compositions (wt.%) of Yamato-75032 and Yamato-74648.

Sample No.	Yamato-75032 low-Ca Pig.			Yamato-75032 Opx.		Yamato-74648
Remarks	Host opx.	Bulk	Aug. blebs	Bulk opx.	Opx.	Opx.
SiO_2	50.8	51.2	48.67	52.5	52.2	53.8
Al_2O_3	0.44	0.54	0.61	0.61	0.67	0.90
TiO_2	0.27	0.37	0.38	0.18	0.20	0.07
Cr_2O_3	0.22	0.44	0.27	0.30	0.32	0.92
FeO	21.35	20.53	8.01	19.47	20.52	16.49
MnO	0.76	0.74	0.62	0.61	0.66	0.58
MgO	22.75	22.42	15.50	23.94	23.69	26.32
CaO	1.16	2.72	22.36	2.10	1.55	1.29
Na_2O	0.00	0.00	0.01	0.00	0.00	0.00
Total	97.75	98.96	96.43	99.71	99.81	100.37
Si	1.945	1.938	1.901	1.950	1.946	1.954
Al	0.020	0.024	0.028	0.027	0.029	0.038
Ti	0.008	0.010	0.011	0.005	0.006	0.002
Cr	0.007	0.013	0.008	0.009	0.009	0.026
Fe	0.684	0.649	0.262	0.605	0.640	0.500
Mn	0.025	0.024	0.021	0.019	0.021	0.018
Mg	1.298	1.264	0.903	1.326	1.316	1.424
Ca	0.048	0.110	0.936	0.084	0.062	0.050
Na	0.000	0.000	0.001	0.000	0.000	0.000
Total	4.035	4.032	4.071	4.025	4.029	4.012
Ca	2.3	5.4	44.6	4.2	3.1	2.6
Mg	64.0	62.5	43.0	65.8	65.2	72.1
Fe	33.7	32.1	12.4	30.0	31.7	25.3

slightly higher in the matrix (Fig. 6). In the matrix, fragments of plagioclase and small chromite and troilite grains are present. The composition of Yamato-75032 chromite is between those of diogenites and eucrites (Fig. 7).

3.2. Discussion

From the above observation combined with other evidence given previously (ISHII and TAKEDA, 1974; TAKEDA and MIYAMOTO, 1977), we suggest that the orthopyroxenes with blebby augites were originally low-Ca pigeonites. In fact, we found the cores of pyroxenes in the Yamato-74450 eucrite to be low-Ca pigeonite as Mg-rich as that of some diogenites (Yamato-74648 in Table 2). By taking into account that Fe/(Fe+Mg) of the Binda pyroxene is almost the same as that of

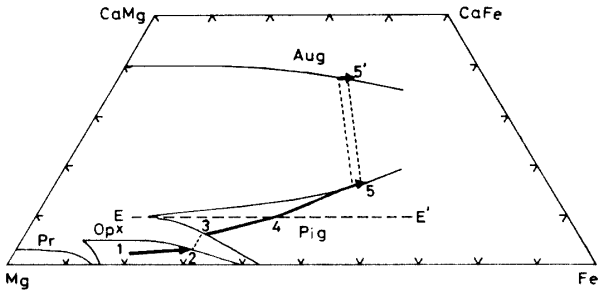

Fig. 8. Pyroxene crystallization sequence of an achondrite parent body projected on an isothermal plane at 1185°C. Phase boundaries of protoenstatite (Pr), orthopyroxene (Opx), pigeonite (Pig), and augite (Aug) are projected on this plane. EE′: projection of the PER line. 1–2: diogenitic orthopyroxenes, 3–4: low-Ca inverted pigeonites, 4–5: pigeonites with the (001) augite lamellae.

Yamato-75032, and that the bulk Ca content (atomic ratio) of Binda and Moama pyroxene is 0.06–0.07 and 0.06–0.08, respectively, we decipher the crystallization trends of the achondrite parent magma as follows (Fig. 8).

The crystallization of orthopyroxenes was followed by pigeonites at around the narrow compositional range between those of Yamato-75032 and Binda. This narrow compositional range implies that the parent liquid compositions as well as temperatures were essentially constant throughout the achondrite crust. In this region, orthopyroxene and pigeonite may coexist. Subsequent to this two-phase region, pigeonite and plagioclase coprecipitate, and the Ca and Fe contents gradually increase until they reach the Moama composition, after which the Ca contents may reach that of the minimum stability field of pigeonite or pigeonite eutectoid reaction (PER) line. We use the term low-Ca pigeonite to refer to a pigeonite with Ca content lower than that at the minimum stability field (*ca.* 8 atom % of Ca). The crystallization of a similar low-Ca pigeonite has been reported in Mull andesite (VIRGO and ROSS, 1973).

The occurrence of low-Ca inverted pigeonite and primary orthopyroxene in Yamato-75032, and the crystallization of low-Ca pigeonite as Mg-rich as diogenitic pyroxenes from a melt with eucritic composition implies a close genetic link between diogenites and eucrites. Diogenitic pyroxenes may crystallize from a eucritic melt with a composition not substantially different from that of Yamato-74450.

4. Eucritic Polymict Breccias

4.1. Results

Yamato-75011 is similar to Yamato-74159 (MIYAMOTO *et al.*, 1978) which is a polymict breccia with a eucritic bulk composition (TAKEDA *et al.*, 1978a). The meteorite contains a variety of pyroxene fragments common to eucrites (Fig. 9)

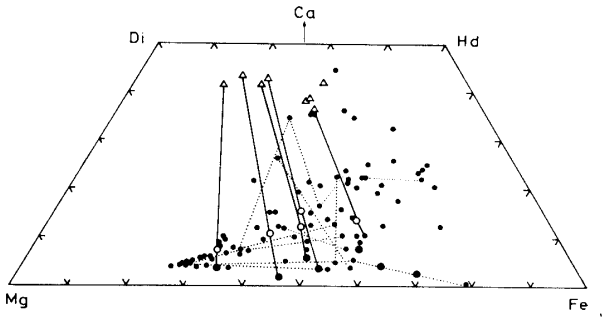

Fig. 9. Pyroxene quadrilateral for the Yamato-75011 polymict breccia. Three different types of pyroxenes are plotted together in different symbols: (1) Pyroxenes with exsolved augites (triangles); open circles indicate bulk compositions, and solid circles, host phase. (2) Chemically zoned pyroxenes. The zoning trend is shown by dots connected by the dotted lines. (3) Pyroxene grains in the matrix (dots).

Table 3a. Selected pyroxene compositions (wt.%) of Yamato-75015.

Remarks	BD			JV		
	Host	Bulk	Aug. blebs	Host	Bulk	Aug. lamella
SiO_2	50.6	49.5	51.5	50.9	50.3	50.9
Al_2O_3	0.61	0.61	0.92	0.69	0.88	1.63
TiO_2	0.28	0.29	0.43	0.48	0.58	0.97
Cr_2O_3	0.30	0.34	0.45	0.31	0.43	0.67
FeO	23.37	22.37	10.91	29.10	26.67	16.26
MnO	0.67	0.85	0.39	0.88	0.84	0.67
MgO	20.70	19.30	14.52	14.40	13.71	11.55
CaO	1.75	3.07	19.71	3.79	6.37	18.12
Na_2O	0.00	0.00	0.00	0.01	0.04	0.11
Total	98.28	96.33	98.83	100.56	99.82	100.88
Si	1.947	1.949	1.955	1.974	1.962	1.935
Al	0.028	0.028	0.041	0.032	0.040	0.073
Ti	0.008	0.009	0.012	0.014	0.017	0.028
Cr	0.009	0.010	0.013	0.010	0.013	0.020
Fe	0.752	0.737	0.347	0.944	0.870	0.517
Mn	0.022	0.028	0.013	0.029	0.028	0.021
Mg	1.188	1.133	0.822	0.832	0.797	0.655
Ca	0.072	0.130	0.802	0.158	0.266	0.738
Na	0.000	0.000	0.000	0.001	0.003	0.008
Total*	4.026	4.024	4.005	3.994	3.996	3.995
Ca**	3.6	6.5	40.7	8.2	13.8	38.6
Mg	59.0	56.7	41.7	43.0	41.2	34.3
Fe	37.4	36.8	17.6	48.8	45.0	27.1

Table 3a (Continued).

Remarks	GBB		GBL	CL21	PM
	Bulk	Aug. lamella	Pig.	Pig.	Pig.
SiO_2	51.4	50.1	51.5	51.1	50.00
Al_2O_3	0.58	1.10	0.69	0.95	1.31
TiO_2	0.41	0.79	0.26	0.17	0.23
Cr_2O_3	0.31	0.53	0.43	0.32	0.64
FeO	23.32	13.47	22.46	25.08	22.04
MnO	0.73	0.62	0.47	0.84	0.79
MgO	18.22	14.71	20.38	19.51	19.61
CaO	5.07	17.03	3.33	2.36	4.35
Na_2O	0.00	0.00	0.00	0.01	0.02
Total	100.04	98.35	99.52	100.34	98.99
Si	1.958	1.927	1.953	1.942	1.917
Al	0.026	0.050	0.031	0.043	0.059
Ti	0.012	0.023	0.007	0.005	0.007
Cr	0.009	0.016	0.013	0.010	0.019
Fe	0.743	0.434	0.712	0.798	0.707
Mn	0.023	0.020	0.015	0.027	0.026
Mg	1.035	0.844	1.151	1.106	1.122
Ca	0.207	0.703	0.135	0.096	0.179
Na	0.000	0.000	0.000	0.001	0.001
Total*	4.013	4.017	4.017	4.028	4.037
Ca**	10.4	35.5	6.8	4.8	8.9
Mg	52.2	42.6	57.6	55.3	55.9
Fe	37.4	21.9	35.6	39.9	35.2

including one Binda-type pyroxene with a few blebs of augite (Fig. 9; Table 3, BD), and basalt fragments with a variety of crystallization textures (Fig. 10a).

Pyroxene fragments show a wide range of exsolution textures. The coarsest exsolution lamella (Table 3, MC) is about 3.5 μm thick with 8.5 μm intervals (Fig. 11a). The finest one resembles that of Juvinas (Table 3, JV). The largest pyroxene clast (0.5 mm in length; Fig. 11b) shows no resolvable lamellae, and has a uniform core with chemical zoning at the margin. This phenocryst-like pigeonite is similar to that found in a monomict breccia Yamato-74450. Plagioclase fragments are present in about equal amount to pyroxene. Silica grains are found rarely in the matrix.

One coarse-grained lithic fragment is composed of parallel laths of alternating

Table 3b. Selected pyroxne compositions (wt.%) of Yamato-75011.

Remarks	BD			MC			JV		
	Host	Bulk	Blebs	Host	Bulk	Lamel-lae	Host	Bulk	Lamel-lae
SiO_2	52.20	51.70	50.90	49.90	49.40	49.50	48.60	48.50	48.00
Al_2O_3	0.69	0.77	1.27	0.55	0.85	2.08	0.66	0.79	1.33
TiO_2	0.59	0.46	0.74	0.41	0.55	1.14	0.62	0.76	1.09
Cr_2O_3	0.42	0.46	0.66	0.21	0.29	0.71	0.11	0.16	0.36
FeO	21.30	20.10	10.03	27.50	24.10	11.38	32.40	30.80	21.30
MnO	0.75	0.69	0.46	1.01	0.84	0.49	0.92	0.94	0.60
MgO	21.90	20.90	14.55	17.57	16.43	12.98	10.99	10.69	9.71
CaO	1.71	3.59	20.20	1.20	4.84	20.00	4.61	6.19	15.22
Na_2O	0.02	0.02	0.16	0.01	0.03	0.11	0.04	0.04	0.13
Total	99.58	98.69	98.97	98.36	97.33	98.39	98.95	98.87	97.74
Si	1.958	1.958	1.930	1.957	1.949	1.930	1.961	1.954	1.952
Al	0.031	0.034	0.057	0.025	0.040	0.094	0.031	0.038	0.063
Ti	0.017	0.013	0.021	0.012	0.016	0.033	0.019	0.023	0.033
Cr	0.012	0.014	0.020	0.007	0.009	0.022	0.004	0.005	0.011
Fe	0.668	0.637	0.318	0.902	0.795	0.366	1.094	1.038	0.714
Mn	0.024	0.022	0.015	0.034	0.028	0.016	0.031	0.032	0.020
Mg	1.225	1.180	0.823	1.027	0.966	0.744	0.661	0.642	0.580
Ca	0.069	0.146	0.821	0.050	0.205	0.824	0.199	0.267	0.654
Na	0.001	0.001	0.012	0.001	0.002	0.008	0.003	0.003	0.010
Total*	4.005	4.005	4.017	4.015	4.010	4.037	4.003	4.002	4.037
Ca**	3.5	7.4	41.8	2.5	10.4	42.6	10.2	13.7	33.6
Mg	62.4	60.1	41.9	51.9	49.1	38.5	33.8	33.0	29.8
Fe	34.1	32.4	16.2	45.6	40.4	18.9	56.0	53.3	36.7

Analysis of Yamato-75011 by M. MIYAMOTO.
* On the basis of O=6.
** Atomic percent.

intergrown plagioclase and pigeonite (Fig. 11c). The fragment is round and resembles an abrasion chondrule described by KING *et al.* (1972) in Pasamonte. The chemical trends of the pyroxenes are also similar to that of Pasamonte but show less extensive Fe–Mg variation. However, Yamato-75011 is much coarser than Pasamonte in grain size. All other mineral fragments also tend to be round rather than angular.

In a portion of one small thin section, which is most likely a portion of a larger lithic clast, there are many skeletal-pyroxene phenocrysts set in a fine, feathery

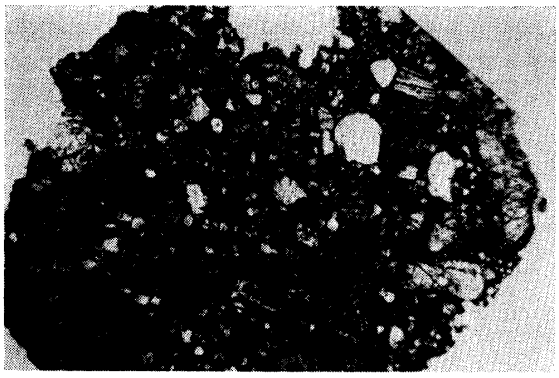

a. Yamato-75011, width 4.3 mm.

b. Abrasion chondrule-like grain with alternating laths of zoned pigeonite and plagioclase in Yamato-75015. Open nicols. Width 4.5 mm.

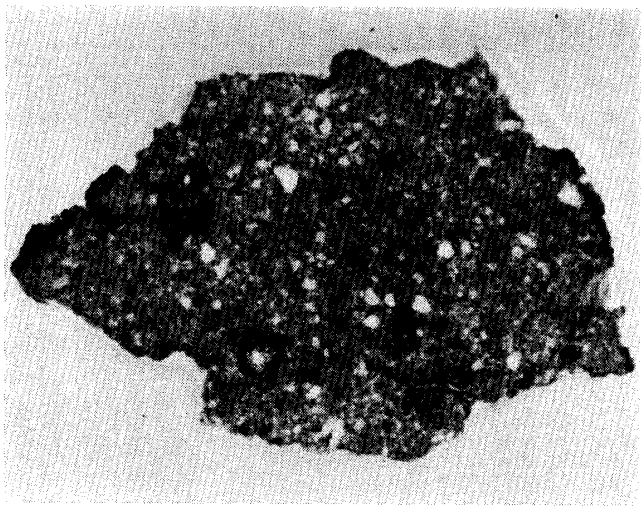

c. Yamato-75015, the largest cut surface, width 20 mm.

Fig. 10. Thin sections of the Yamato-75 eucritic polymict breccia, showing fragments with variety of lithic clasts and mineral fragments known to eucrites. Open nicols.

dark matrix (Fig. 11d). The texture is similar to some of the lunar mare basalts, and to Yamato-74450. The texture of Yamato-74450 is apparently porphyritic, with equant clinopyroxene phenocrysts incorporated into a plagioclase-clinopyroxene intergrowth. The groundmass of Yamato-74450 is more coarsely crystalline than that of the clast in Yamato-75011.

Yamato-75015 is another polymict breccia with a eucritic composition. The bulk chemistry obtained by fused bead analyses (M. B. DUKE, private communication) is the same as that of Yamato-74159 (TAKEDA *et al.*, 1978a) and common eucrites. The texture (Figs. 10b and 10c) and the mineral assemblages and pyroxene chemical trends (Figs. 12a–12c) are also similar to those of Yamato-75011. One

a. Pyroxene fragment with the coarsest exsolution lamellae in Yamato-75011.

b. The largest pyroxene clast of the Pasamonte-type in Yamato-75011.

c. Abrasion chondrule-like particle in Yamato-75011. Alternating laths of intergrown plagioclase and pigeonite show chemical zoning.

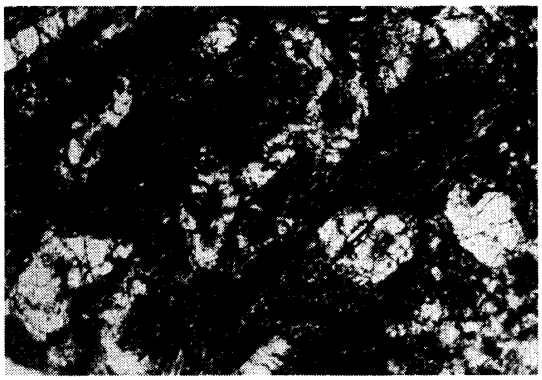

d. A lithic clast with hollow-core skeletal-pyroxene phenocrysts set in a fine feathery dark matrix.

Fig. 11. Photomicrographs (open nicols) of individual pyroxene fragments and lithic clasts in Yamato-75011. Width 0.95 mm.

small difference lies in the observation that Yamato-75015 contains fragments of slightly more slowly cooled pyroxenes than those in Yamato-75011.

Lithic clasts are not as common as those in Yamato-74159. Spherically shaped alternating parallel laths of intergrown plagioclase-pigeonite (Figs. 10b and 13a) are not uncommon, and were also observed in Yamato-75011. The largest such clast found in Yamato-75015 has an elliptical shape (2.5×1.3 mm). Pigeonites and plagioclases in these clasts show chemical zoning of the Pasamonte-type pyroxenes (Fig. 12c). A pigeonite in a coarse-grained chondrule-like grain 0.65×0.88 mm in size has uniform Mg-rich core (PM in Table 3) with Fe-enrichment at the plagioclase boundary (PM in Table 4) (Fig. 13a).

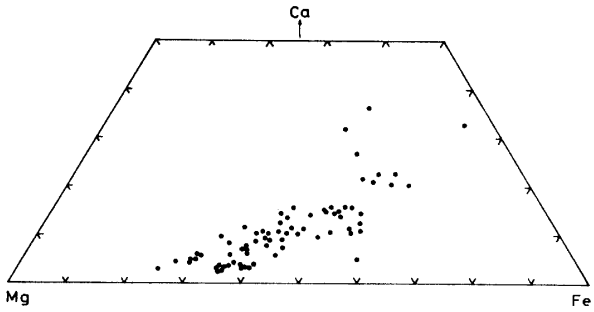

a. General chemical trends of pyroxene compositions in Yamato-75015, including grains both in the clasts and matrices.

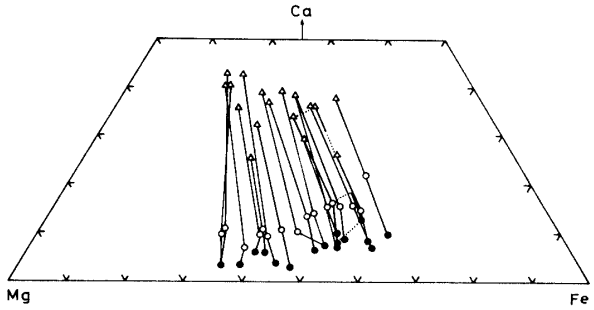

b. Chemical compositions of pyroxene crystal fragments with exsolution lamellae of augite. Open circles: bulk compositions; solid circles: compositions of the host phases; triangles: lamellae augites; lines connect the lamella and host pairs.

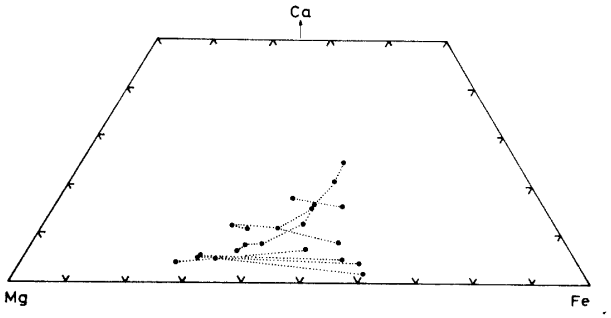

c. Chemical zonings of pyroxene fragments and pyroxenes in the lithic clasts of the Pasamonte-type.

Fig. 12. Pyroxene quadrilaterals for Yamato-75015, a eucritic polymict breccia.

Other clast-types found within the thin sections include a metal-troilite-rich spherical grain 0.8 mm in diameter, and a clast (1.0 mm in diameter) with plagioclase crystals scattered in a dark matrix (Fig. 10c).

Pyroxene fragments in the matrix have a range of colors from colorless and yellowish to gray brown, pinkish brown and reddish brown. They can be

a. An enlarged portion of Fig. 10b. Open nicols.

b. Pyroxene clast with the Moama-like exsolution texture. Crossed nicols.

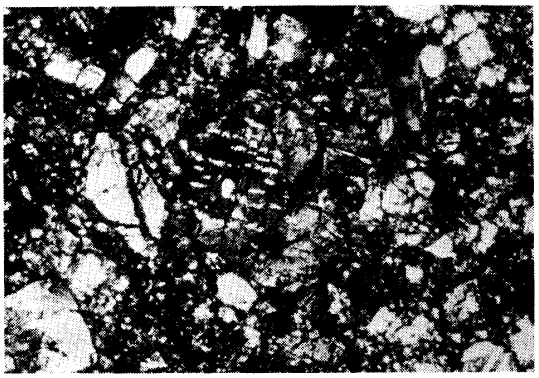

c. Pyroxene fragment with the Binda-like exsolution texture. Numbers of blebs are smaller than those of Fig. 13b. Crossed nicols.

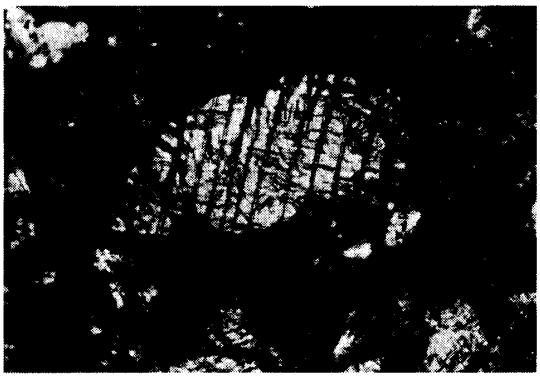

d. Pyroxene crystal with the coarsest exsolution lamellae.

e. Lithic fragment in which a pyroxene with coarse exsolution lamellae is in contact with plagioclase by a smoothly curved boundary.

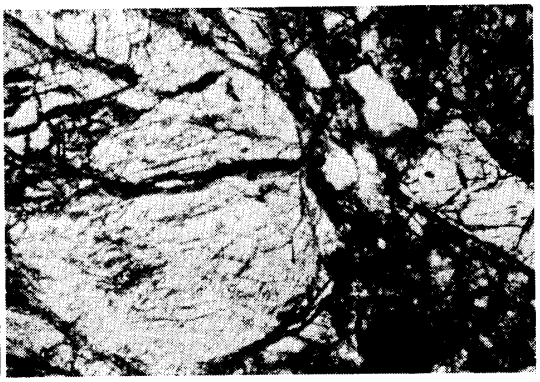

f. Large pyroxene fragment with nearly uniform Mg-rich composition but with no exsolution lamellae.

Fig. 13. Photomicrographs of individual pyroxene fragments and lithic clasts in Yamato-75015. c-axes nearly horizontal. Width 0.95 mm.

classified into four types: The Binda-type (BD) of pyroxene with blebby oriented augites, the Moore County-like (MC) pyroxenes with coarse exsolution lamellae of augite with (001) in common, the Juvinas-type (JV) brownish pigeonite with fine exsolution textures, and the Pasamonte-type (PM) pigeonite with no visible exsolution lamellae.

The largest BD-type pyroxene reaches 1.45×0.90 mm in size (Fig. 13b). The texture of this grain resembles that of Moama pyroxene, but it has not been confirmed whether the host pyroxene is orthopyroxene or pigeonite. Another grain 0.31×0.38 mm in size (BD in Table 3a and Fig. 13c) has few blebs, the width of the blebs being about 3 μm with about 12 μm intervals. The chemical composition of the BD-type pyroxene is uniform within grains and do not differ from grain to grain. The BD-type pyroxene is one of the most Mg-rich members in this breccia and its composition falls between the Binda and Moama pyroxenes.

The MC-type pyroxenes are characterized by their widely separated thick lamellae, although they are not as thick as those in Moore County (MASON, 1962). The largest grain (Fig. 13d) has 9 μm wide lamella with 35 μm intervals. This type of pyroxene has been found in Yamato-74159 and Yamato-75011, but no lithic clasts containing such pyroxenes have been identified. Two plagioclase fragments in Yamato-75015 have a fragment of the MC-type pyroxene attached at a smoothly curved boundary (Fig. 13e and GBB, GBL in Table 3a).

The JV-type pyroxenes exhibit a brownish color, and fine regular exsolution lamellae on (001). The largest crystal reaches 0.5×0.75 mm in size. The width of the lamellae is about a few μm with the same interval as the lamellae. The JV-type pyroxenes are higher in Fe and Ca than those of the other types.

The bulk chemistry of the above three types of pyroxenes together with their host and lamella pairs cover a wide range in the pyroxene quadrilateral (Fig. 12b). The chemical trends of pyroxene in Yamato-75015 delineate the crystallization path postulated in Fig. 8. The chemical compositions of individual pyroxene fragments in the matrix (Fig. 12a) are also distributed in the same way as in Fig. 8.

On the other hand, there are a number of large pyroxene fragments which do

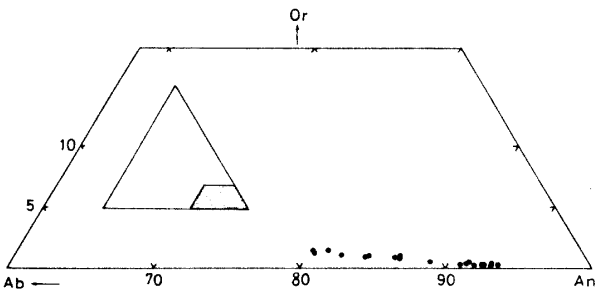

Fig. 14. The Or–Ab–An percentages of the plagioclase clasts in Yamato-75015. The shaded portion is enlarged.

not fit into the above pattern. The largest fragment of such pyroxenes reaches 1.4×0.7 mm in size, and has a nearly uniform Mg-rich composition (CL21 in Table 3a). No visible exsolution lamellae are found in these pyroxenes, but some of them contain oriented opaque mineral inclusions (Fig. 13f).

Plagioclase fragments are also abundant, the largest one being 0.55×0.65 mm. The Or–Ab–An percentages of the plagioclase clasts are given in Fig. 14, and the chemical compositions of plagioclase grains which occur in contact with pyroxenes in some lithic clasts are given in Table 4 (GBB, GBL). Other minor minerals in-

Table 4. Selected plagioclase composition (wt.%) of Yamato-75015.

Remarks	GBB Bulk	GBL Cont.	PM Core	PM Variolitic
SiO_2	44.3	45.0	47.3	48.7
Al_2O_3	34.9	34.6	32.5	30.6
TiO_2	0.00	0.00	0.01	0.00
Cr_2O_3	0.01	0.00	0.01	0.00
FeO	0.49	0.18	0.61	1.07
MnO	0.00	0.00	0.00	0.00
MgO	0.09	0.05	0.15	0.00
CaO	18.90	18.55	17.03	15.99
Na_2O	0.73	0.97	1.60	1.92
K_2O	0.05	0.05	0.14	0.21
Total	99.47	99.40	99.35	98.49
Si	2.063	2.090	2.192	2.272
Al	1.914	1.894	1.774	1.682
Ti	0.000	0.000	0.000	0.000
Cr	0.001	0.000	0.000	0.000
Fe	0.019	0.007	0.024	0.042
Mn	0.000	0.000	0.000	0.000
Mg	0.006	0.004	0.010	0.000
Ca	0.942	0.923	0.846	0.799
Na	0.066	0.087	0.144	0.174
K	0.003	0.003	0.008	0.013
Total*	5.014	5.008	4.998	4.982
K**	0.3	0.3	0.8	1.3
Na	6.5	8.6	14.4	17.6
Ca	93.2	91.1	84.8	81.1

* On the basis of O=8.
** Atomic percent.

Table 5. Chemical data on chromites, ilmenites, and a silica mineral in Yamato-75015 (wt.%).

Minerals	Chromite		Ilmenite		SiO_2
	1	2	1	2	
SiO_2	0.09	0.11	0.08	0.05	99.0
Al_2O_3	16.54	8.73	0.04	0.03	0.55
TiO_2	1.21	5.02	51.8	51.7	0.17
Cr_2O_3	46.20	47.12	0.01	0.82	0.00
FeO	33.9	36.1	45.6	45.1	0.08
MnO	0.71	0.76	0.93	0.87	0.00
MgO	0.93	0.60	0.80	0.78	0.00
CaO	0.02	0.05	0.10	0.03	0.09
Na_2O	0.02	0.00	0.00	0.00	0.00
V_2O_3	0.40	0.68	0.28	0.30	0.00
Total	100.02	99.17	99.64	99.68	99.89
Si	0.02	0.03	0.004	0.003	0.993
Al	5.34	2.95	0.002	0.002	0.006
Ti	0.25	1.08	1.969	1.962	0.001
Cr	10.00	10.67	0.001	0.033	0.000
Fe	7.77	8.66	1.927	1.902	0.001
Mn	0.16	0.18	0.040	0.037	0.001
Mg	0.38	0.26	0.060	0.059	0.000
Ca	0.01	0.01	0.005	0.002	0.001
Na	0.01	0.00	0.000	0.000	0.000
V	0.09	0.16	0.012	0.012	0.000
Total	24.03	24.00	4.020	4.012	1.003
O	32	32	6	6	2

clude chromite, ilmenite, and a silica mineral (1.0×0.5 mm). Their compositions are given in Table 5.

4.2. Discussion

Because both Yamato-75011 and -75015 contain all types of eucritic materials as was found in Yamato-74159 (MIYAMOTO *et al.*, 1978), the interpretation given in that paper is also applicable to these meteorites. It is interesting to note that abrasion chondrules with coarse-grained texture are found in two meteorites. If the Mg-rich pigeonite fragments without exsolved augite can be interpreted as fragments of the core pyroxene of the Pasamonte-type, all the pyroxenes in these meteorites may be considered as a brecciated product of a layered crust model.

A model for the layered crust will be explained in detail below.

5. The Yamato-74659 and -74123 Ureilite

This meteorite originally weighed 18.9 g, but a considerable portion of the meteorite has been used for an unknown purpose before this identification. This meteorite was brought to the curator's attention because of its unusual appearance, and a small fragment was analyzed by standard wet chemical methods (Table 6) by Mr. H. HARAMURA of the University of Tokyo. The results indicated that its chemical composition matches weathered ureilites. The total carbon analysis by E. GIBSON (private communication, 1978) gave C=3.03 wt.%.

It is the ninth known ureilite (MIYAMOTO *et al.*, 1978; HUTCHINSON, 1977). The elemental composition of Yamato-74659 is different from the other ureilites (BERKLEY *et al.*, 1978) in that the FeO content (8.83 wt.%) is the lowest among the known ureilites and it is richer in SiO_2 (42.91 wt.%). The composition is con-

Table 6. Bulk compositions (wt. %) of the Yamato-74659 ureilite.

Element	Yamato-74659	Range of ureilite**
SiO_2	42.91	36.8–41.9
TiO_2	0.14	0.12–0.18
Al_2O_3	1.07	0.32–0.87
Fe_2O_3	1.47	
FeO	8.83	14.5–21.1
MnO	0.42	0.361–0.384
MgO	38.78	36.7–39.2
CaO	1.71	0.4–1.4
Na_2O	0.07	0.03–0.05
K_2O	<0.02	42 (ppm)
$H_2O(-)$	0.17	
$H_2O(+)$*	3.65	
P_2O_5	0.14	
FeS	0.49	
Fe		
Ni	0.14	900–2300 (ppm)
Co	<0.003	80–139 (ppm)
Cr_2O_3	0.64	0.66–0.78
Total	100.653	

Analysis by H. HARAMURA, 1977.

* Volatiles released at 1100°C, including C.

** After MASON, 1971, except SiO_2.

Table 7. Chemical compositions of pigeonites and olivines from the Yamato-74659 ureilite.

Remarks	Pigeonite				Olivines
	1	2	3	3 ave.	Core
SiO_2	57.8	56.4	56.6	56.0	39.7
Al_2O_3	0.26	0.48	0.55	0.58	0.03
TiO_2	0.10	0.10	0.14	0.14	0.01
Cr_2O_3	0.34	0.84	0.83	0.85	0.53
FeO	2.76	5.52	5.46	5.47	8.49
MnO	0.50	0.46	0.47	0.46	0.45
MgO	33.3	32.8	34.22	32.2	50.8
CaO	4.10	3.82	2.44	3.84	0.32
Na_2O	0.15	0.06	0.03	0.07	0.02
Total	99.31	100.48	100.74	99.61	100.35
Si	1.997	1.957	1.951	1.960	0.970
Al	0.011	0.020	0.022	0.024	0.001
Ti	0.003	0.003	0.004	0.004	0.000
Cr	0.009	0.023	0.023	0.024	0.010
Fe	0.080	0.160	0.157	0.160	0.174
Mn	0.014	0.013	0.014	0.014	0.009
Mg	1.718	1.699	1.760	1.681	1.851
Ca	0.152	0.142	0.090	0.144	0.008
Na	0.010	0.004	0.002	0.005	0.001
Total	3.994	4.021	4.023	4.016	3.024
Ca*	7.8	7.1	4.5	7.2	0.4
Mg	88.1	84.9	87.7	84.7	91.1
Fe	4.1	8.0	7.8	8.1	8.5

* Atomic %.

sistent with the fact that it is composed of one of the most Mg-rich pigeonites $Ca_7Mg_{85}Fe_8$ and Mg-rich olivines $Fa_{7.9}$, and that the amount of pigeonite is larger than olivine. Olivine grains (Fig. 15) forming triple point junctures display minor difference in their Fa contents. A round pigeonite grain enclosed entirely in olivine gives the lowest Ca concentration (Table 7, pigeonite 3). X-ray diffraction studies of a pigeonite crystal did not show any evidence of exsolution of augite, inversion to orthopyroxene, or twinning. A widely spaced fine lineation that was previously thought to represent twin bands parallel to (100) was found to be not the case. They bear resemblance to fractures nearly parallel to (001) produced by the high-low inversion of pigeonite or parting. The diffraction spots are broad,

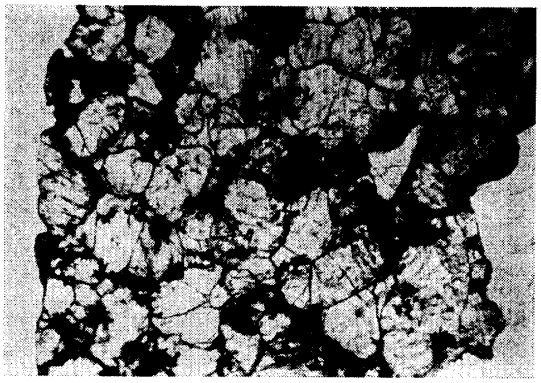

Fig. 15. Photomicrograph of the Yamato-74659. Width 4.0 mm.

indicating shock effects. The thermal history of Yamato-74659 must be constrained such that the growth of pyroxenes and olivines with nearly uniform composition was followed by shock events and rapid cooling.

The Yamato-74123 previously included in chondrite on the basis of the olivine compositions has been identified as ureilites. The distribution of the olivine compositions resembled that of the H3 chondrites. The previous measurements were done only on a few grains of olivine. The variation of the iron contents of the olivines is due to the chemical zoning produced by reduction. The new observation done on a larger thin section indicated that the Yamato-74123 ureilite is similar to Kenna in its texture and compositions. The most common composition of olivine is $Ca_{0.5}Mg_{79}Fe_{20.5}$, and that of pigeonite $Ca_{6.6}Mg_{75}Fe_{18.4}$.

6. A Layered Crust Model for an Achondrite Parent Body

MASON (1967) proposed a model of a differentiated asteroid with eucritic crust, diogenitic mantle, and pallasitic core. Crystallographic features of the achondritic pyroxenes such as exsolution and inversion textures vary sequentially in accordance with Fe/(Mg+Fe) ratios in their crystallization trend. On the basis of such features, we can place individual achondrites at various depths within the primordial crust. The details of data and reasonings in support of the following model have been published in part in our previous papers (TAKEDA *et al.*, 1976; TAKEDA and MIYAMOTO, 1977; TAKEDA, 1977; TAKEDA *et al.*, 1978b). A reference documenting how the various exsolution textures can be correlated to p–T conditions has been given by ISHII and TAKEDA (1974). However, minor revisions may be required on the basis of Fig. 8. A roughly estimated depth within the crust for each meteorite has been derived from the widths of exsolved pyroxenes by application of diffusion theories and computer simulation (MIYAMOTO and TAKEDA, 1977). Here we present our interpretation as a hypothetical working model for a better understanding of the data of the Yamato-75 achondrites. They can be

arranged from bottom to top as:

(a) Very low calcium, magnesium-rich orthopyroxenes. The composition of some pyroxenes may approach those in Steinbach, although Steinbach is not a diogenite.

(b) Medium calcium and magnesium-rich orthopyroxenes with no exsolution of augite (*e.g.* Shalka), or more calcium-rich and iron-rich orthopyroxenes with augite exsolution lamellae with (100) in common (*e.g.* Ibbenbüren) or both. Developments of exsolution lamellae in these pyroxenes of rather low calcium contents compared to terrestrial plutonic pyroxenes suggests that the exsolution was developed deeper in the crust than other varieties (ISHII and TAKEDA, 1974).

(c) The last diogenite crystallized in the sequence may contain orthopyroxenes with blebby augites or low-calcium inverted or decomposed pigeonites, such as found in Yamato-75032.

(d) Inverted or decomposed pigeonites of 'low-calcium' content (see Section 3.2.) with blebby augites with (100) in common (*e.g.* Binda). Plagioclase starts to crystallize at this stage. The temperature of the point where the crystallization trend reaches the lower stability limit of pigeonite or pigeonite eutectoid reaction (PER) line was estimated to be above 1100°C (ISHII, 1975).

(e) Inverted pigeonites of high bulk calcium content with coarse exsolution lamellae of augite with (001) in common (*e.g.* Moore County). In some cases, pigeonite has only partially inverted to orthopyroxene. It coexists with equigranular plagioclase grains.

(f) Common eucritic pigeonites with uniform composition and with fine exsolved augite lamellae with (001) in common (*e.g.* Juvinas). The host phase is clinohypersthene. Plagioclase and pyroxene show ophitic to subophitic texture.

(g) Pasamonte-like pigeonites with extensive chemical zoning from magnesium-rich pigeonite to ferrohedenbergite. Exsolution is detected only by the X-ray diffraction (TAKEDA *et al.*, 1976). Plagioclase is needle-like or radiated together with the pyroxenes. Because this kind of zoning is expected to be produced by crystallization from a supercooled melt, this type of eucrite may represent a surface lava or impact melt.

7. Discussion

All the achondrites described in this paper display one or two uncommon features compared to known achondrites. Yamato-75032 is the most Fe-rich diogenite known to date, and is composed of both low-Ca inverted pigeonite and orthopyroxene. Yamato-75011 contains a clast containing skeletal pigeonite phenocrysts. Yamato-75015 is a breccia which contains all types of pyroxenes known to eucrites. The first finding of the Binda-like inverted pigeonite in a eucritic polymict breccia is reported. The Yamato-74659 achondrite, tentatively

identified as a weathered ureilite, contains the most Mg-rich pigeonite known.

It should be noted that there are two different Mg-rich pyroxene clasts in the eucritic polymict breccias. Because the two kinds of pyroxene occur as large fragments and their chemical compositions are nearly uniform, they may be misidentified as fragments of Fe-rich diogenitic pyroxenes. However one type of pyroxene has blebby augite inclusions in the host pyroxene with a uniform bulk composition, and the other type of pyroxene is a slightly zoned pigeonite with Fe-enrichment at the very margin. We interpret the latter fragments as originally representing a part of the core of the PM-like pyroxenes.

The occurrence of the BD-like pyroxenes in polymict breccias has been expected from the layered crust model. They may represent the first pyroxene crystallized in the crystallization sequence of the eucritic crust (3 to 4 in Fig. 8). Because such pyroxenes are presumably found deepest in the eucritic crust, Yamato-75011 and -75015 may contain all types of materials in a layered eucritic crust. The crystallization of the BD-like pyroxenes in the diogenite Yamato-75032, also supports the crystallization sequence proposed in Fig. 8.

The distribution of the bulk chemical compositions of all pyroxenes is depicted in the crystallization sequence shown in Fig. 8. Although the location of the PER line (EE′ in Fig. 8) is not precisely known, pigeonites crystallized from 3 to 4 in Fig. 8 contain blebby augites of the BD-type. The pigeonites to the right of 4 show much coarser exsolution textures than the more Fe-rich members around 5. One question that needs to be answered is why the true Moore County-like pyroxenes with very coarse exsolution lamellae (*ca.* 50 μm) in the partially inverted host phase have not been found in any eucritic polymict breccia. Also, the fact that the residual materials of the partial melting model of STOLPER (1977) have not been found in any polymict breccia may give more support to a model involving accretional processes which will be explained below. Perhaps these "residues" if ever existed may be located too deep to be incorporated into most breccias.

The finding of a diogenite-like meteorite (Yamato-75032) with a pyroxene composition close to that of Binda emphasizes the important genetic link between eucrites and diogenites. There is no apparent gap (difference) between the pyroxene crystallization trends of eucrite and diogenite. The occurrence of pigeonite in diogenites implies that transitional crystallization of pigeonite from orthopyroxene took place before the simultaneous crystallization of plagioclase and pigeonite and that the occurrence of pigeonite cannot be a diagnostic criterion of eucrites. Again, diogenites and eucrites represent two portions, fortuitously divided, of a continuous spectra of pyroxenes in a pyroxene crystallization trends of these genetically related achondrites.

The model proposed previously (TAKEDA *et al.*, 1976; TAKEDA, 1977) explains the pyroxene crystallization sequence and their relative locations within the pro-

posed crust, and does not necessarily imply that they are produced by large scale crystal fractionation from a totally molten crust with a hypothetical composition. Our model is compatible with the partial melting model for eucrites proposed by STOLPER (1977), since the melt produced by the large scale partial melting is our initial molten crust.

All the previous models did not take into account a process of actual crust formation on the parent body. We have proposed a new model (TAKEDA, 1977) involving accretional processes for producing the layered crust, by taking into account all reasonable processes proposed for both the partial melting and the crystal fractionation models. It consists of four typical stages.

(A) Initial stage of partial melting by accretional heating. When the size of the parent body reaches a certain value, materials on the surface will begin to melt by heat generated by accreting or impacting particles as was proposed for the moon (MIZUTANI *et al.*, 1972; KAULA, 1978). Since the size of an achondrite parent body is assumed to be smaller than that of the moon and larger than that of Vesta (about 1000 km in diameter), an additional heating such as short-lived radiogenic heating and induction heating by the protosun etc. may be required to melt only the surface of a small body. The melts may be equivalent to more advanced partial melts of STOLPER (1977), that were multiply saturated with olivine, pyroxene and plagioclase, with olivine in reaction relationship.

(B) Melting of accreting or impacting materials, while crystallizing cumulate-type diogenites and eucrites. The surface of the molten layer is still being heated by accretion, while the bottom is cooled by conduction of heat towards the colder interior. The crystallization will proceed as postulated by a crystal fractionation model, but the composition of the melt will be maintained or buffered near the peritectic point (olivine-pyroxene-plagioclase) by constant supply of materials by accretion and their large scale partial melting.

Because this accretion and melting took place at a very early stage of the planetary formation within a limited region of the solar system, the sizes of the accreting materials may not be too large, and their compositions may not vary too much. At the last stage, thickness of the molten layer becomes so large that the amounts and sizes of the accreting materials and their compositions may not affect the condition of the molten layer. During the crystallization, the residues of partially molten accreted materials and fractionated crystals may react with well stirred melts to produce diogenitic pyroxenes and a melt that is not far from the peritectic point. Therefore the most of the residues will be consumed leaving the diogenitic materials.

(C) End of accretion and rapid cooling of the molten layer. As soon as accretion stops, the temperature of the surface decreases very rapidly, because there may be no other effective heat source such as the radiogenic one on the small parent body. This rapid cooling will produce the Pasamonte-type eucrite on the

very surface. The interior of the residual liquid layer also cools rapidly, producing unfractionated common eucrites.

(D) Brecciation and mixing of the surface materials by a subsequent impact, to produce howardites and eucritic polymict breccias.

The crystallization sequence and cooling histories of pyroxenes of the above model may be postulated as below. Because the depths and extensions of the molten layer are assumed to be planetary in scale, we have to admit that there are some local modifications. However, since the correlation between the chemical compositions of pyroxenes and their exsolution and inversion textures is high (see Section 6), we expect the sequences may be represented by those given in Fig. 8. This schematic figure shows a projection of phase boundaries and the crystallization trends onto an equithermal plane at about 1180°C. The EE′ line is the projection of the pyroxene eutectoid reaction (PER) line (ISHII, 1975).

The line from 1 (1180°C) to 2 represents the crystallization of diogenitic pyroxenes. From 2 to 3 (*ca.* 1165°C), the crystallization of orthopyroxene is taken over by low-Ca pigeonite. We tentatively define pyroxenes crystallizing from 3 to 4 (1150°C) as low-Ca pigeonite. The pigeonites crystallizing after 4 may reach the stable pigeonite-augite solvus, producing the platy lamellae of augite with (001) in common (ISHII and TAKEDA, 1974), whereas those before 4 may reach the metastable extension of the solvus, or decompose into pigeonite+orthopyroxene or pigeonite+orthopyroxene+augite before reaching the solvus upon slow cooling. The textures of these slowly cooled pyroxenes may be represented by those in Binda or Moama. The pigeonites beyond 4 represented by many common eucrites show more rapidly cooled exsolution textures than Moama. Augites crystallizing in cotectic relationship with pigeonites at 5 (*ca.* 1130°C) are rare in eucrites.

The ureilite pyroxenes show chemical proximity to the diogenitic ones among achondrites other than the genetically related ones. However, the structure and exsolution and inversion textures of the Yamato-74659 pyroxene are entirely unrelated to those of the diogenitic pyroxenes.

Since the newly found eucritic polymict breccias may represent brecciated products of our proposed layered crust, their reflectance spectrum should match that of the asteroid 4 Vesta. This conclusion is consistent with that reached by LEBERTRE and ZELLNER (1978) who reported the resemblance of Vesta's reflectance spectrum with that of powdered mixtures of various eucrites. Thus the detailed studies of the Yamato eucritic polymict breccias will provide information on the surface materials of the differentiated asteroids.

Acknowledgments

We thank members of the field party of the Japanese Antarctic Research Expedition in 1975 for collecting the meteorites, and Mr. H. HARAMURA of the

University of Tokyo for allowing us to quote his analysis of Yamato-74659, and Dr. E. GIBSON of NASA-JSC for his carbon analysis. We are indebted to Dr. M. B. DUKE, Dr. Brian MASON, Mr. E. STOLPER, Profs. R. SADANAGA, Y. TAKÉUCHI, N. ONUMA and K. ITO for discussion and interest. A part of this study has been supported by a Fund for Scientific Research of the Ministry of Education, Scince and Culture, and Itoh Science Foundation grant. We thank Dr. Brian MASON, Prof. K. KEIL and Dr. J. L. BERKLEY for critically reading the manuscript and Miss M. SATO for helping us with microprobe analyses.

References

BERKLEY, J. L., TAYLOR, G. J. and KEIL, K. (1978): Ureilites: Origin as related magmatic cumulates. Lunar and Planetary Science IX. Houston, Lunar and Planetary Institute, 73–75.

DRAKE, M. J. and CONSOLMAGNO, G. J. (1977): Asteroid 4 Vesta: Possible bulk composition deduced from geochemistry of eucrites (abstract). Lunar Science VIII. Houston, Lunar Science Institute, 248–250.

DUKE, M. B. and SILVER, L. T. (1967): Petrology of eucrites, howardites and mesosiderites. Geochim. Cosmochim. Acta, **31**, 1637–1665.

HUTCHINSON, R. (1977): A crystalline ureilite from Oman. Meteoritics, **12**, 263.

ISHII, T. (1975): The relation between temperature and composition of pigeonite in some lavas and their application to geothermometry. Mineral. J., **8**, 48–57.

ISHII, T. and TAKEDA, H. (1974): Inversion, decomposition and exsolution phenomena of terrestrial and extraterrestrial pigeonites. Mem. Geol. Soc. Jpn, **11**, 19–36.

KAULA, W. M. (1978): Planetary thermal evolution during accretion. Lunar and Planetary Science IX. Houston, Lunar and Planetary Institute, 615–617.

KING, E. A. Jr., BUTLER, J. C. and CARMAN, M. F. (1972): Chondrules in Apollo 14 samples and size analyses of Apollo 14 and 15 fines. Proc. 3rd Lunar Sci. Conf., 673–686 (Geochim. Cosmochim. Acta, Suppl. **3**).

LEBERTRE, T. and ZELLNER, B. (1978): The surface texture of Vesta. Lunar and Planetary Science IX. Houston, Lunar and Planetary Institute, 642–644.

MASON, B. (1962): Meteorites. New York, Wiley, 274 p.

MASON, B. (1976): Meteorites. Am. Sci., **55**, 429–455.

MATSON, D. L., FANALE, F. P., JOHNSON, T. V. and VEEDER, G. L. (1976): Asteroids and comparative planetology. Proc. 7th Lunar Sci. Conf., 3603–3627 (Geochim. Cosmochim. Acta, Suppl. 7).

MATSUMOTO, Y. (1978): Collection of Yamato meteorites, East Antarctica in November and December 1975, and January 1976. Mem. Natl Inst. Polar Res., Spec. Issue, **8**, 38–50.

MIYAMOTO, M. and TAKEDA, H. (1977): Evaluation of a crust model of eucrites from the width of exsolved pyroxenes. Geochem. J., **11**, 161–169.

MIYAMOTO, M., TAKEDA, H. and YANAI, K. (1978): Yamato achondrite polymict breccias. Mem. Natl Inst. Polar Res., Spec. Issue, **8**, 185–197.

MIZUTANI, H., MATSUI, N. and TAKEUCHI, H. (1972): Accretion process of the Moon. Moon, **4**, 472–484.

NAKAMURA, Y. and KUSHIRO, I. (1970): Compositional relations of coexisting orthopyroxene, pigeonite and augite in a tholeiitic andesite from Hakone volcano. Contrib. Mineral. Petrol., **26**, 265–275.

OKADA, A. (1975): Petrological studies of the Yamato meteorites. Part 1. Mineralogy of the Yamato meteorites. Mem. Natl Inst. Polar Res., Spec. Issue, **5**, 91–110.

STOLPER, E. (1977): Experimental petrology of eucritic meteorites. Geochim. Cosmochim. Acta, **41**, 587–611.

TAKEDA, H., MIYAMOTO, M., ISHII, T. and REID, A. M. (1976): Characterization of crust formation on a parent body of achondrites and the moon by pyroxene crystallography and chemistry. Proc. 7th Lunar Sci. Conf., 3535–3548 (Geochim. Cosmochim. Acta, Suppl. **7**).

TAKEDA, H. (1977): Genetic relationship of diogenites and eucrites and its parent body. Proc. 10th Lunar and Planetary Symp. Tokyo, Inst. Space Aero. Sci., Univ. of Tokyo, 47–52.

TAKEDA, H. and MIYAMOTO, M. (1977): Inverted pigeonites from lunar breccia 76255 and pyroxene-crystallization trends in lunar and achondritic crusts. Proc. 8th Lunar Sci. Conf., 2617–2626 (Geochim. Cosmochim. Acta, Suppl. **8**).

TAKEDA, H., MIYAMOTO, M., YANAI, K. and HARAMURA, H. (1978a): A preliminary mineralogical examination of the Yamato-74 achondrites. Mem. Natl Inst. Polar Res., Spec. Issue, **8**, 170–184.

TAKEDA, H., MIYAMOTO, M., DUKE, M. B. and ISHII, T. (1978b): Crystallization of pyroxenes in lunar KREEP basalt 15386 and meteoritic basalts. Proc. 9th Lunar Planet. Sci. Conf., 1157–1171 (Geochim. Cosmochim. Acta, Suppl. **9**).

VIRGO, D. and ROSS, M. (1973): Pyroxenes from Mull andesites. Carnegie Inst. Washington, Yearb., **72**, 535–540.

YAGI, K., LOVERING, J. F., SHIMA, M. and OKADA, A. (1978): Mineralogical and petrographical studies of the Yamato meteorites, Yamato-7301(j), -7305(k), -7308(l) and -7303(m) from Antarctica. Mem. Natl Inst. Polar Res., Spec. Issue, **8**, 121–141.

YANAI, K., MIYAMOTO, M. and TAKEDA, H. (1978): A classification for the Yamato-74 chondrites based on the chemical compositions of their olivines and pyroxenes. Mem. Natl Inst. Polar Res., Spec. Issue, **8**, 110–120.

(Received June 12, 1978; Revised manuscript received October 31, 1978)